International Journal of Environment, Agriculture and Biotechnology
Vol-11, Issue-3; May-Jun, 2026
Peer-Reviewed International Journal
Journal Home Page Available: https://ijeab.com/
Journal DOI: 10.22161/ijeab

Spatiotemporal Dynamics and Drivers of Daytime and Nighttime Urban Heat Islands in the Guangdong-Hong Kong-Macao Greater Bay Area: Insights from XGBoost-SHAP

Shiya Feng, Ruei-Yuan Wang*

School of Sciences, Guangdong University of Petrochem Technology (GDUPT), Maoming 525000, China

Received: 16 May 2026; Received in revised form: 14 Jun 2026; Accepted: 17 Jun 2026; Available online: 24 Jun 2026

Abstract**—** *The Guangdong-Hong Kong-Macao Greater Bay Area (GBA) is a representative region in China characterized by a high level of urbanization, rapid land-use changes, and intensive population and economic activities. Identifying the spatiotemporal patterns and driving factors of daytime and nighttime surface urban heat island (SUHI) intensity is of great significance for regional thermal environment management and territorial spatial planning. Based on multi-source datasets from 2018 to 2024, this study developed an analytical framework consisting of "SUHI pattern identification–land-use transition response–driving mechanism interpretation" to reveal the evolution and driving mechanisms of the thermal environment in the GBA from a diurnal perspective. The results showed that: (1) High SUHI values during both daytime and nighttime were concentrated in core built-up areas such as Guangzhou, Foshan, Dongguan, and Shenzhen, whereas low-value areas were mainly distributed in mountainous forest regions in the north and coastal water bodies along the Pearl River Estuary. (2) From 2018 to 2024, SUHI intensity exhibited overall fluctuations, with an increasing trend in the eastern urban corridor of the Pearl River Delta, whereas the northwestern mountainous areas remained relatively stable or experienced a slight decline. (3) The conversion of forestland, cropland, and water bodies/wetlands to construction land significantly intensified SUHI, with the strongest warming effect observed when water bodies/wetlands were converted to construction land. Conversely, the transformation of construction land into green spaces or water bodies effectively mitigated SUHI. (4) XGBoost-SHAP analysis revealed that NDBSI, NDVI, NDMI, MNDWI, and NTL were the key factors influencing daytime SUHI, whereas NDBSI, NTL, PD (population density), GDP, and NDVI were the primary drivers of nighttime SUHI. These findings provide a scientific basis for thermal environment regulation, urban expansion control, and blue-green space conservation in the GBA.*

Keywords**— *Guangdong-Hong Kong-Macao Greater Bay Area (GBA); Surface Urban Heat Island (SUHI); Daytime and Nighttime Differences; Land-use Transition; XGBoost-SHAP Model***

I. INTRODUCTION

The urban heat island (UHI) effect is one of the most prominent thermal environmental problems associated with rapid urbanization and is closely linked to changes in urban land surfaces, alterations in surface energy balance, and increasing anthropogenic heat emissions (Oke, 1987). With the continuous expansion of built-up areas, the increase in impervious surfaces, the reduction of vegetation cover, and the intensification of human activities, urban regions experience substantial changes in energy exchange processes, hydrothermal conditions, and heat storage capacity. These changes often result in significantly higher surface temperatures in urban areas

than in surrounding ecological landscapes, thereby intensifying the surface urban heat island (SUHI) effect.

The GBA, comprising Guangzhou, Shenzhen, Zhuhai, Foshan, Huizhou, Dongguan, Zhongshan, Jiangmen, Zhaoqing, Hong Kong, and Macao, is one of the most densely urbanized and economically dynamic urban agglomerations in China. The region contains highly concentrated built-up areas while simultaneously preserving extensive ecological spaces, including mountains, forests, wetlands, rivers, and coastal water bodies. This unique spatial configuration provides an ideal setting for investigating the spatiotemporal dynamics and driving mechanisms of daytime and nighttime SUHIs at the urban agglomeration scale. Over the past decade, the GBA has experienced rapid urban expansion, increasing population and industrial concentration, and substantial changes in land-use structure. Meanwhile, the region is located within a typical subtropical monsoon climate zone characterized by frequent high-temperature and high-humidity conditions. The interaction between accelerated urbanization and complex natural environments has intensified thermal environmental challenges across the region. Consequently, understanding the formation mechanisms, spatial heterogeneity, and evolution of SUHIs has become increasingly important for climate adaptation, urban planning, ecological conservation, and public health protection. Recent studies have emphasized several critical issues, including daytime–nighttime differences in SUHI mechanisms, anthropogenic heat contributions, heatwave-related risks, urban ventilation constraints, environmental justice concerns, and the cooling thresholds of blue–green infrastructure. These emerging topics indicate a shift in UHI research from simple pattern description toward comprehensive thermal risk assessment and management.

Existing UHI studies have mainly focused on three aspects. First, investigations of spatiotemporal SUHI patterns have widely employed thermal infrared remote sensing data, such as MODIS and Landsat imagery, revealing that high-intensity SUHI areas are generally concentrated in densely built-up regions, whereas forests, wetlands, and water bodies provide significant cooling effects (Chen et al., 2006). Second, studies on land-use change have demonstrated that urban expansion is a major contributor to thermal environmental deterioration, while ecological restoration can effectively mitigate SUHI intensity (Liu et al., 2014). Third, with advances in machine learning techniques, increasing attention has been devoted to identifying the driving mechanisms of thermal environments. Models such as Random Forest and Extreme Gradient Boosting (XGBoost) have proven effective in capturing complex nonlinear relationships among environmental variables and SUHI intensity (Yang et al., 2022).

Previous studies have further demonstrated that land-use transitions exert substantial influences on regional thermal environments. The conversion of ecological land into built-up land is often accompanied by increasing surface temperatures and intensified SUHI effects (Liu et al., 2014). At the global scale, rapid urban expansion has significantly strengthened SUHI intensity, although considerable regional differences remain (Zhou et al., 2017). Conversely, increases in vegetation coverage and water bodies can effectively alleviate thermal stress through evapotranspiration and cooling effects, thereby serving as important ecological regulators of urban climate (Li et al., 2020). In recent years, machine learning approaches have increasingly been adopted to explore SUHI formation mechanisms, revealing complex nonlinear interactions among climatic, ecological, socioeconomic, and landscape factors (Yang et al., 2022). Studies conducted in the GBA have also reported significant spatial clustering of SUHIs, with hotspots predominantly concentrated in the highly urbanized core areas of the Pearl River Delta (Wang et al., 2023).

Despite these advances, several important limitations remain. First, most studies focus on a single temporal dimension and rarely provide systematic comparisons between daytime and nighttime SUHI dynamics. Second, quantitative assessments of the relationships between land-use transitions and SUHI evolution remain limited, particularly at the urban agglomeration scale. Third, existing studies on driving mechanisms often emphasize variable importance rankings while paying insufficient attention to the nonlinear response characteristics and threshold effects of key influencing factors. Furthermore, integrated investigations linking SUHI patterns, land-use transitions, and driving mechanisms within a unified analytical framework remain scarce. These limitations hinder a comprehensive understanding of thermal environmental evolution in rapidly urbanizing regions. To address these gaps, this study aims to answer three key research questions: (1) Where are the SUHI hotspots in the GBA, how have they evolved from 2018 to 2024, and do they exhibit significant spatial clustering characteristics? (2) How is major land-use transition pathways associated with increases or decreases in daytime and nighttime SUHI intensity? (3)Which environmental, socioeconomic and landscape factors play dominant roles in shaping daytime and nighttime SUHIs, and how do their effects differ?

Using multi-source spatial datasets from 2018 to 2024, this study investigates the spatiotemporal evolution,

land-use transition responses, and driving mechanisms of daytime and nighttime SUHIs in the GBA. The relationships among research questions, analytical methods, and expected outputs are summarized in Table 1. Specifically, RQ1 examines the spatiotemporal distribution and spatial clustering characteristics of daytime and nighttime SUHIs; RQ2 quantifies the thermal environmental impacts of land-use transitions; and RQ3 identifies the dominant driving factors and their nonlinear response mechanisms. Together, these three research questions constitute a progressive analytical framework of "pattern identification–process response–mechanism explanation," providing a comprehensive understanding of SUHI evolution in one of the world's most rapidly urbanizing regions.

Table 1 Research Questions and Analytical Framework

Research Questions/Pattern Recognition	Corresponding method/process response	Expected Output/Mechanism Explanation
RQ1: Exploring the spatiotemporal patterns of diurnal and nocturnal SUHI?	Interannual statistics, trend analysis, Global Moran's I, LISA	Spatial distribution of SUHI, trend enhancement zones, hot/cold spots
RQ2: How does land-use transfer affect SUHI?	Land-use transfer matrix, ΔSUHI analysis	Main transfer pathways and their warming/cooling effects
RQ3: What are the primary drivers of diurnal SUHI?	XGBoost, SHAP	Variable importance, direction of effect, nonlinear response

II. STUDY AREA AND METHODS

2.1 Overview of the Study Area

The study area is the Guangdong–Hong Kong–Macao Greater Bay Area (GBA) (Figure 1), which consists of nine cities in the Pearl River Delta and the two Special Administrative Regions of Hong Kong and Macao. Located along the southern coast of China, the GBA lies within a typical subtropical monsoon climate zone characterized by warm temperatures, abundant precipitation, and distinct wet and dry seasons. The region features diverse topography, including plains, hills, mountains, river networks, and coastal waters.

As one of the most economically dynamic and highly urbanized regions in China, the GBA serves as a key growth pole in the national strategy for regional coordinated development. Between 2018 and 2024, rapid urban expansion, population growth, and industrial agglomeration led to substantial changes in land-use patterns, particularly the continuous increase in built-up land and the transformation of ecological spaces. These changes have significantly influenced the regional thermal environment.

The GBA contains both highly urbanized metropolitan areas, such as Guangzhou, Shenzhen, and Dongguan, and extensive ecological spaces, including the mountainous forests in the northern region, the Pearl River water system, and coastal wetlands. This diverse landscape creates pronounced spatial heterogeneity in land cover, urban development intensity, and ecological functions, making the region well suited for investigating the interactions among urbanization, land-use change, and surface thermal environments.

Given its rapid urbanization, complex natural conditions, and diverse land-use characteristics, the GBA provides an ideal case for examining the spatiotemporal evolution of daytime and nighttime SUHIs, their responses to land-use transitions, and the underlying driving mechanisms at the urban agglomeration scale.

2.2 Data Sources and Preprocessing

The data used in this study include six categories of variables: thermal environment, land-use, ecological moisture, built-up dry surfaces, topographic climate, and socio-economic activities (Table 2 and Table 3). Thermal environment data were employed to construct diurnal SUHI; land-use data were used to analyze land cover structure and transition processes; NDVI (Normalized Difference Vegetation Index), NDMI (Normalized Difference Moisture Index), NDWI (Normalized Difference Water Index), and MNDWI (Modified Normalized Difference Water Index) were utilized to characterize vegetation, moisture, and water body cooling capacity; NDBSI (Normalized Difference Built-up Index) was applied to represent built-up, bare, and dry surfaces; DEM, Slope, ATP (Temperature), PRE (Precipitation) and SPI (Standardized Precipitation Index) were used to depict natural topography and climatic hydrothermal conditions; while NTL (Nighttime Light Index), PD (Population Density), and GDP (Gross Domestic Product) served as indicators of human activities, population agglomeration, and economic activity intensity.

All remote sensing and environmental variables underwent data retrieval, quality control, annual compositing, study area clipping, spatial alignment, and scale unification on the Google Earth Engine (GEE) platform. Socio-economic variables were assigned to unified spatial analysis units based on administrative boundaries. To avoid false precision issues, this study organized multi-source variables using a unified analytical grid. High-resolution land-use data were aggregated using the majority method, continuous variables were aggregated using the mean method, and administrative statistical variables were assigned through spatial joins.

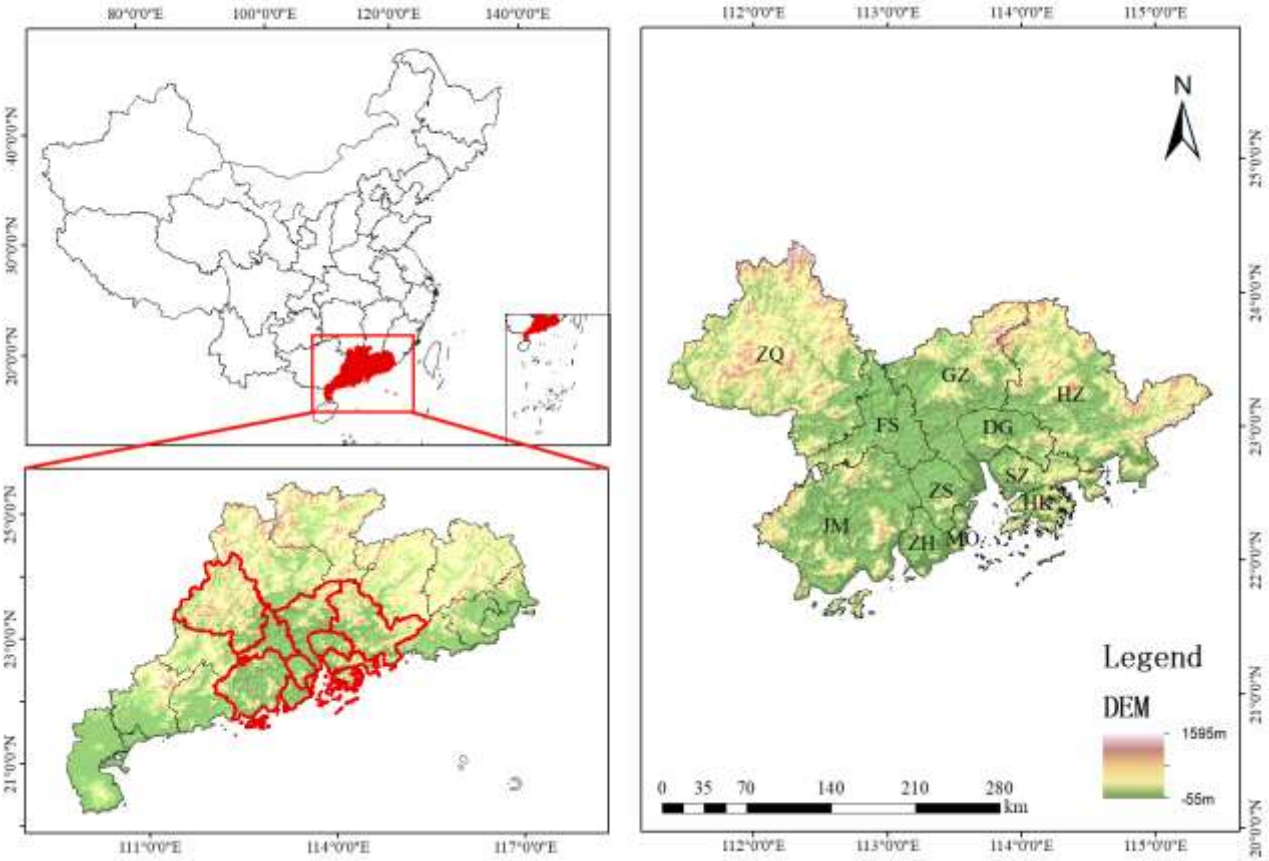

Fig.1 Location Map of the Study Area

Table 2 Research Variables and Their Descriptions

Data Category	Variable	Purpose
Thermal environment	LST_Day, LST_Night, SUHI_Day,SUHI_Night	Constructing daytime and nighttime SUHI intensity
Land-use	LULC	Identify land-use structure and transition pathways
Ecological moisture	NDVI,NDMI,NDWI,MNDWI	Characterizing the cooling effects of vegetation, moisture, and water bodies
Dry surface	NDBSI	Characterization of hardened, bare, and dry surfaces
Terrain and climate	DEM, Slope, ATP, PRE, SPI	Characterizing natural background and climatic hydrothermal conditions
Socio-economic activities	NTL, PD, GDP	Characterizing the intensity of human activities, population, and economic agglomeration

Table 3 Data Sources and Basic Information

Data Category	Data Product	Time range	Resolution	Data Source
LST	MOD11A2	2018–2024	1 km	Download from the GEE platform
LULC	ESA WorldCover	2018–2024	10 m	
NDVI	MOD13Q1	2018–2024	250 m	
NDMI	Landsat 8/9	2018–2024	30 m	
NDWI	Landsat 8/9	2018–2024	30 m	
MNDWI	Landsat 8/9	2018–2024	30 m	
NDBSI	Landsat 8/9	2018–2024	30 m	
DEM	SRTM	None	30 m	
Slope	Calculate from DEM	None	30 m	
ATP	ERA5-Land	2018–2024	0.1°	
PRE	CHIRPS	2018–2024	0.05°	
SPI	Calculate from CHIRPS	2018–2024	0.05°	
NTL	VIIRS VNL	2018–2024	500 m	
PD	WorldPop	2018–2024	100 m	
GDP	China Urban Statistical Yearbook	2018–2024	Municipal level	National Bureau of Statistics（https://www.stats.gov.cn/）

2.3 Methodology

This study constructs a daytime–nighttime SUHI intensity database for the GBA covering the period from 2018 to 2024, based on multi-source remote sensing, natural environmental, and socio-economic data. A comprehensive analysis is conducted from three perspectives: spatiotemporal evolution, land-use transition responses, and driving mechanism identification.

First, daytime and nighttime SUHI indicators are developed using land surface temperature (LST) data. Interannual statistical analysis and trend analysis are employed to reveal temporal variations in heat island intensity. Global Moran's I and Local Indicators of Spatial Association (LISA) are applied to identify SUHI hotspots, cold spots, and their spatial clustering characteristics.

Second, land-use transition matrices are used to characterize conversion processes among different land-use types. By integrating ΔSUHI analysis, the impacts of various land-use transitions on thermal environmental changes are assessed, thereby identifying dominant warming and cooling transition patterns.

Finally, multidimensional driving factors, including vegetation, moisture, built environment, topographic and climatic conditions, and socio-economic activities, are incorporated into the analysis. The XGBoost machine learning model is employed to quantify the contribution of each factor to daytime and nighttime SUHI intensity, while SHAP-based interpretation methods are used to reveal the directional effects, influence magnitudes, and nonlinear response relationships of key drivers. This framework systematically elucidates the formation mechanisms and evolutionary patterns of daytime and nighttime heat island effects in the GBA, as illustrated in Figure 2.

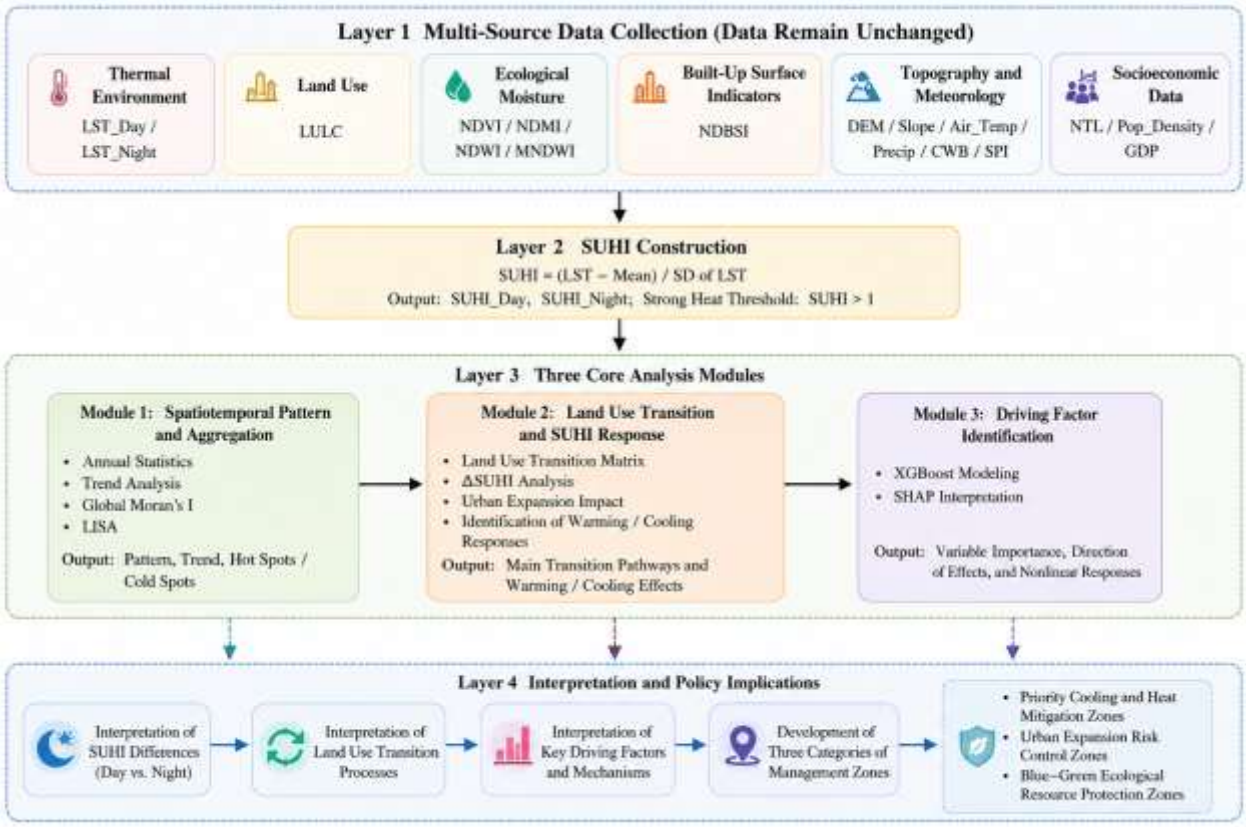

Fig.2. The Framework of the Study

2.3.1 SUHI Indicator Construction

This study employs the Standardized SUHI Intensity to characterize the deviation of different spatial units within the study area from the regional average thermal environment in a given year. Daytime and nighttime SUHIs are calculated separately, as shown in equations (1) and (2):

Daytime:

$$SUHI_i^{day} = (LST_i^{day} - mean(LST^{day}))/SD(LST^{day}) \quad (1)$$

Nighttime：

$$SUHI_i^{night} = (LST_i^{night} - mean(LST^{night}))/SD(LST^{night}) \quad (2)$$

In equations (1) and (2), $SUHI_i$ represents the urban heat island intensity of the ith spatial unit, LST_i denotes the land surface temperature of that spatial unit, mean (LST) indicates the annual average land surface temperature of the study area, and $SD(LST)$ represents the standard deviation of the land surface temperature in the study area for that year. Standardization processing can reduce the impact of climatic background differences across different years on the comparison of heat island intensity.

Based on the standardized SUHI Intensity values, the study area was classified into five categories (Table 4). Areas with SUHI values below −1.0 were defined as strong cold island (SCI) zones, indicating surface temperatures significantly lower than the regional average and typically corresponding to ecological cooling sources such as forests and water bodies. Regions with SUHI values ranging from −1.0 to −0.5 were classified as weak cold island (WCI) zones, exhibiting a certain degree of cooling effect. Areas with SUHI values between −0.5 and 0.5 were categorized as neutral zones (NZ), where thermal conditions were close to the regional average. Areas with SUHI values ranging from 0.5 to 1.0 were defined as weak heat island (WHI) zones, reflecting surface temperatures higher than the regional average. Meanwhile, areas with SUHI values greater than 1.0 were classified as strong heat island (SHI) zones, indicating significant heat accumulation and typically concentrated in urban core built-up areas and high-intensity development zones.

Table 4 SUHI Classification Criteria

Scope	Level	Explanation
SUHI < -1.0	Strong Cold Island (SCI) zones	Significantly lower than the regional average thermal environment
-1.0 ≤ SUHI < -0.5	Weak Cold Island (WCI) zones	Lower temperature zone
-0.5 ≤ SUHI ≤ 0.5	Neutral zones (NZ)	Close to the regional average
0.5 < SUHI ≤ 1.0	Weak Heat Island (WHI) zones	Higher temperature zone
SUHI > 1.0	Strong Heat Island (SHI) zones	Significantly higher than the regional average thermal environment

2.3.2 Spatiotemporal Patterns and Spatial Aggregation Analysis of Daytime and Nighttime SUHI

First, the mean value, standard deviation, proportion of strong heat island areas, and proportion of strong cold island areas of daytime and nighttime SUHI in different years were calculated to characterize overall thermal environment changes during the study period. Second, linear trend analysis was performed for each spatial unit to identify areas experiencing SUHI intensification or weakening. A positive trend slope indicates SUHI intensification, whereas a negative trend slope indicates SUHI weakening.

Furthermore, Global Moran's I was used to examine whether daytime and nighttime SUHI exhibited overall spatial autocorrelation (Equation 3). A significantly positive Moran's I value indicates that high values tend to cluster with high values and low values tend to cluster with low values in space. Subsequently, Local Indicators of Spatial Association (LISA) were employed to identify local spatial aggregation patterns (Equation 4), including High–High hotspot areas, Low–Low cold spot areas, High–Low outlier areas, and Low–High outlier areas.

Global Moran's I:

$$I = \frac{N}{\sum_{i=1}^{N}\sum_{j=1}^{N} w_{ij}} \times \frac{\sum_{i=1}^{N}\sum_{j=1}^{N} w_{ij}(x_i - \bar{x})(x_j - \bar{x})}{\sum_{i=1}^{N}(x_i - \bar{x})^2}$$

(3)

Local Moran's I:

$$I_i = \frac{(x_i - \bar{x})}{\frac{1}{n}\sum_{k=1}^{n}(x_k - \bar{x})^2} \cdot \sum_{j=1}^{n} w_{ij}(x_j - \bar{x})$$

(4)

In equations (3) and (4), I represents the Global Moran's I index; n is the number of sample units; w_{ij} denotes the spatial weight matrix; W is the sum of all spatial weights; x_i and x_j represent the SUHI values of spatial units i and j, respectively; $\bar{x}$ is the mean SUHI value of the study area. The range of Moran's I is [-1, 1]. A value greater than 0 indicates positive spatial correlation, less than 0 indicates negative spatial correlation, and a value close to 0 suggests a random spatial distribution.

2.3.3 Analysis of Land-Use Transitions and Their SUHI Responses

Land-use transition matrices were constructed based on land-use/land-cover (LULC) maps from 2018 and 2024 to quantify the direction and magnitude of land-use changes during the study period. The transition matrix provides a quantitative representation of conversion relationships among different land-use categories and has been widely applied in land-change dynamics analysis (Pontius et al., 2004; Liu et al., 2014).

To reveal the influence of land-use transformation on surface thermal environments, a land-use transition matrix was generated based on the initial and final years of the study period. In the matrix, Tij represents the area converted from land-use type (i) to land-use type (j) between 2018 and 2024. This approach allows the identification of dominant transformation pathways and their corresponding thermal responses.

Particular attention was given to transition pathways associated with the conversion of ecological land into built-up areas, including forestland, cropland, water bodies, wetlands, and bare land converted into impervious surfaces. Meanwhile, transitions from built-up areas to ecological spaces, such as green spaces and water bodies, were also examined to evaluate potential cooling effects associated with ecological restoration and urban renewal.

Considering that SUHI intensity reflects relative thermal anomalies rather than absolute temperature differences, the variation in SUHI intensity (ΔSUHI) was calculated for each spatial unit to characterize thermal environmental changes between 2018 and 2024 (Equation 5).:

$$\Delta SUHI_i = SUHI_i2024 - SUHI_i2018 \quad (5)$$

Where $\Delta SUHI_i$ represents the change in SUHI intensity for spatial unit (i); $SUHI_i2024$ and $SUHI_i2018$

represent the standardized SUHI values in 2024 and 2018, respectively. Positive ΔSUHI values indicate increasing thermal anomalies, suggesting a warming effect associated with land-use change, whereas negative values indicate cooling effects. Subsequently, the average ΔSUHI values corresponding to different land-use transition pathways were calculated to identify which transformation processes contributed to SUHI intensification or mitigation (Table 5).

Table 5 Land Use Transition Pathways and Expected Thermal Environment Effects

Transfer path	Thermal environmental effect	Explanation
Forestland/Cropland →Built-up land	SUHI enhancement	Reduced vegetation, increased hardening, weakened evapotranspiration
Water bodies/wetlands →Built-up land	SUHI enhancement	The cooling effect of water bodies is weakening
Bare land →Built-up land	May enhance	Surface heat storage and increase in impervious surfaces
Built-up Land → Green space/Water body	SUHI weakened	Enhanced ecological cooling and humidification conditions
Stable Built-up land	Maintain high SUHI	High thermal storage and intense human activity
Stable Forestland/Water bodies	Maintain low SUHI	Stable cooling source and evapotranspiration

2.3.4 XGBoost-SHAP Factor Identification

To identify the key factors influencing diurnal SUHI, this study constructed separate XGBoost regression models for daytime SUHI and nighttime SUHI. As a machine learning method based on gradient-boosted decision trees, XGBoost can effectively capture nonlinear relationships and complex interactions among high-dimensional variables (Chen & Guestrin, 2016). The dependent variables were $SUHI_{Day}$ and $SUHI_{Night}$, while the explanatory variables included LULC, NDVI, NDMI, NDWI, MNDWI, NDBSI, DEM, Slope, ATP, PRE, SPI, NTL, PD and GDP.

An Extreme Gradient Boosting (XGBoost) model was employed to capture the nonlinear relationships between urban heat island intensity and multi-source driving factors. The XGBoost prediction is formulated as (6):

$$\hat{y}_i = \phi(\mathbf{x}_i) = \sum_{k=1}^{K} f_k(\mathbf{x}_i) + b_0 \quad (6)$$

where $\hat{y}_i$ is the predicted SUHI at location i, xi is the vector of explanatory variables (e.g., NDVI, impervious surface ratio, nightlight index), fk is the kth regression tree, and b0is the base score. To interpret the XGBoost model, SHapley Additive exPlanations (SHAP) values were computed using the Tree SHAP algorithm (Lundberg & Lee, 2017), the formulated as (7):

$$\phi_j^{(i)} = \sum_{S \subseteq F \setminus \{j\}} \frac{|S|!(|F|-|S|-1)!}{|F|!} [f(S \cup \{j\})(x_i) - f(S)(x_i)] \quad (7)$$

The prediction for sample i can be decomposed as $\hat{y}_i = \phi_0 + \sum_{j=1}^{n} \phi_j^{(i)}$, where $\phi_j^{(i)}$ denotes the local contribution of the jth driver. Global feature importance was assessed as the mean absolute SHAP value, $\frac{1}{n}\sum_{i=1}^{n} |\phi_j^{(i)}|$."

XGBoost provides an additive predictive modeling framework, while SHAP values offer mathematically interpretable measures of the contribution of each driving factor to the predicted outcome. The combination of these two methods constitutes the complete theoretical foundation for "XGBoost-SHAP driver identification." XGBoost is used to model the nonlinear relationships between multidimensional variables and SUHI, whereas SHAP explains the model outputs by quantifying the marginal contribution of each variable to the predictions.

This study focuses on analyzing SHAP variable importance, SHAP summary plots, and dependence plots of key variables to determine which factors are most influential, whether their contributions to SUHI are positive or negative, and whether threshold effects or nonlinear response relationships exist. To enhance model generalization and reduce random sampling errors, the model training process adopts a 70% training set and 30% test set split, combined with five-fold cross-validation (5-fold cross-validation) for parameter optimization. In each cross-validation iteration, the training samples are divided into five subsets, with four subsets used for model training and the remaining subset used for validation. This process is repeated until all validation rounds are completed.

Model performance is evaluated using the coefficient of determination (R^2), root mean square error (RMSE), and mean absolute error (MAE). The R^2 value measures the model's explanatory power for SUHI variations, while

RMSE and MAE are used to assess prediction error levels. An R^2 value closer to 1 indicates a better model fit, whereas lower RMSE and MAE values indicate higher prediction accuracy.

Based on the parameter optimization results, the final XGBoost model parameters are set as follows: number of trees (n_estimators) = 300, maximum tree depth (max_depth) = 6, learning rate (learning_rate) = 0.05, subsample ratio (subsample) = 0.8, feature subsample ratio (colsample_bytree) = 0.8, and random seed (random_state) = 42. This configuration ensures prediction accuracy while effectively mitigating overfitting.

III. RESULTS

3.1 Spatiotemporal Distribution and Trends of Daytime and Nighttime SUHI

From 2018 to 2024, the GBA exhibited a spatial pattern characterized by "high values in the center and low values in the periphery" for both daytime and nighttime SUHI Intensity. High-SUHI areas were primarily concentrated in the core urban agglomerations of the Pearl River Delta, including highly urbanized regions such as Guangzhou, Shenzhen, Dongguan, and Foshan, forming continuous heat island cores. In contrast, low-SUHI areas were mainly distributed in the northern mountainous and hilly regions, as well as coastal water bodies such as the Pearl River Estuary and Lingdingyang. In 2018, high-SUHI zones had already formed distinct clusters within the built-up areas of the Guangzhou–Foshan and Shenzhen–Dongguan metropolitan regions. Subsequently, with continued urban development and the expansion of built-up land, these high-SUHI areas further extended into surrounding regions, although the overall spatial pattern remained relatively stable. Meanwhile, the northern forested areas and coastal waters consistently maintained low SUHI levels, exhibiting stable cold island characteristics.

Significant differences were observed between the spatial distributions of daytime and nighttime SUHI. During the daytime, high-SUHI areas were more extensive, extending beyond urban cores to encompass surrounding industrial zones and towns, thereby forming large contiguous heat island regions. Low-SUHI areas predominantly corresponded to ecological land-cover types such as forests and water bodies (Figure 3). In contrast, nighttime high-SUHI areas were more concentrated and were primarily located within central business districts and high-density built-up areas of cities such as Guangzhou and Shenzhen. Although the spatial extent of nighttime heat islands was considerably smaller than that observed during the daytime, their spatial clustering characteristics were more pronounced (Figure 4). Overall, daytime heat island effects exhibited stronger spatial diffusion, whereas nighttime heat island effects showed more evident core clustering, reflecting the persistent influence of urban surface heat storage and delayed nocturnal heat release on the thermal environment (Figure 5).

Trend analysis revealed that SUHI dynamics in the GBA from 2018 to 2024 exhibited significant spatial heterogeneity. In the northwestern portion of the study area, including mountainous regions such as Zhaoqing, SUHI generally remained stable or showed a weakening trend. In contrast, the eastern Pearl River Delta, particularly the Shenzhen–Dongguan–Huizhou urban development corridor, experienced a pronounced intensification of SUHI, forming a continuous warming belt. Combined with land-use distribution patterns and statistical results, these findings indicate that the core Pearl River Delta region, characterized by highly contiguous built-up land, extensive impervious surface coverage, and intensive population and industrial activities, experienced sustained heat accumulation and storage, resulting in persistent high-SUHI zones. Conversely, the northern mountainous forest regions, with dense vegetation cover and strong evapotranspiration effects, effectively reduced surface temperatures, while coastal water bodies, influenced by high thermal capacity and sea–land breeze circulation, formed stable cold island zones. Consequently, the study area gradually developed a thermal environmental pattern in which urban agglomerations functioned as heat sources, while mountainous forests and coastal waters served as cooling sources.

Table 6 presents the overall statistical characteristics of daytime and nighttime SUHI in the GBA from 2018 to 2024. Because SUHI was calculated using Z-score standardization, the mean value of the study area theoretically approached zero. Accordingly, the average SUHI remained approximately −0.03 throughout the study period, indicating a relatively stable overall thermal environmental distribution among years. In contrast, the standard deviation and the proportion of strong heat island areas more effectively reflected spatial variations in thermal environmental conditions. The standard deviation of daytime SUHI ranged from 1.74 to 2.10, substantially higher than that of nighttime SUHI (1.28–1.74), indicating greater spatial heterogeneity in daytime surface thermal conditions. Furthermore, the proportion of strong daytime heat island areas (4.58%–9.69%) was markedly higher than that of nighttime heat island areas (0.42%–1.84%), demonstrating that daytime heat island effects were stronger and more spatially extensive, whereas nighttime heat island effects were primarily concentrated within core

built-up areas. Overall, the thermal environment of the GBA exhibited distinct diurnal differences: daytime surface temperatures were more strongly influenced by solar radiation and surface characteristics, whereas nighttime temperatures primarily reflected urban heat storage and anthropogenic heat emissions.

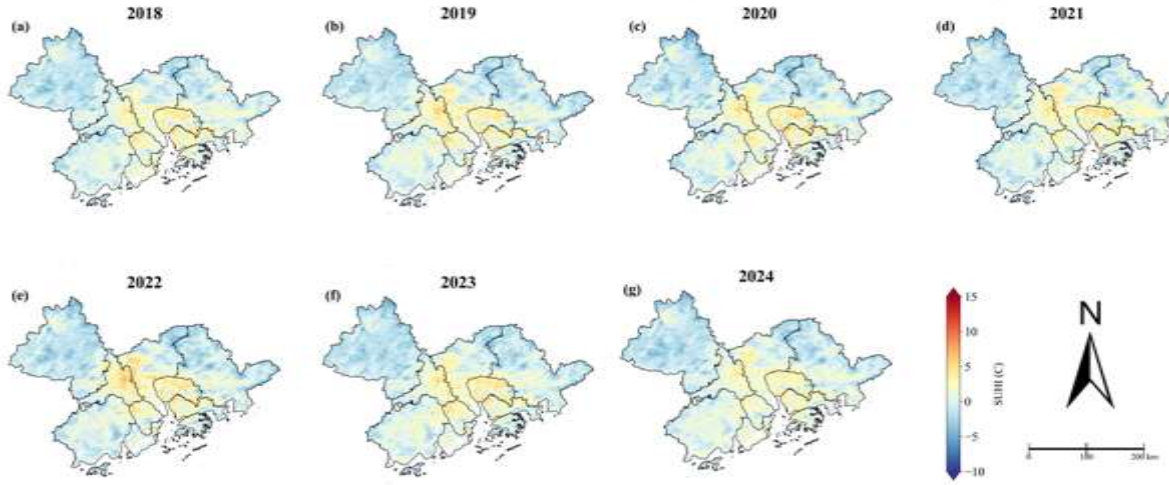

Figure 3 Spatial Distribution of Daytime SUHI from 2018 to 2024

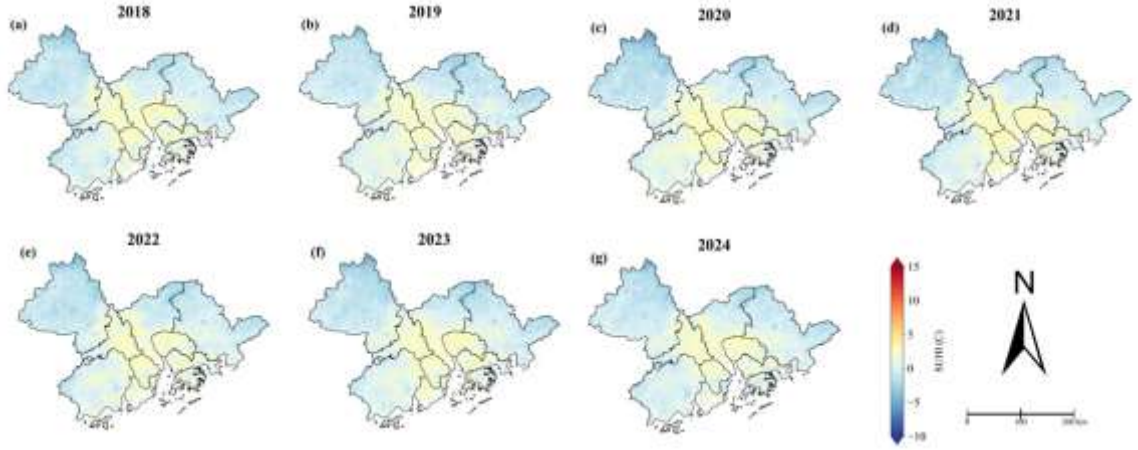

Figure 4 Spatial Distribution of Nighttime SUHI from 2018 to 2024

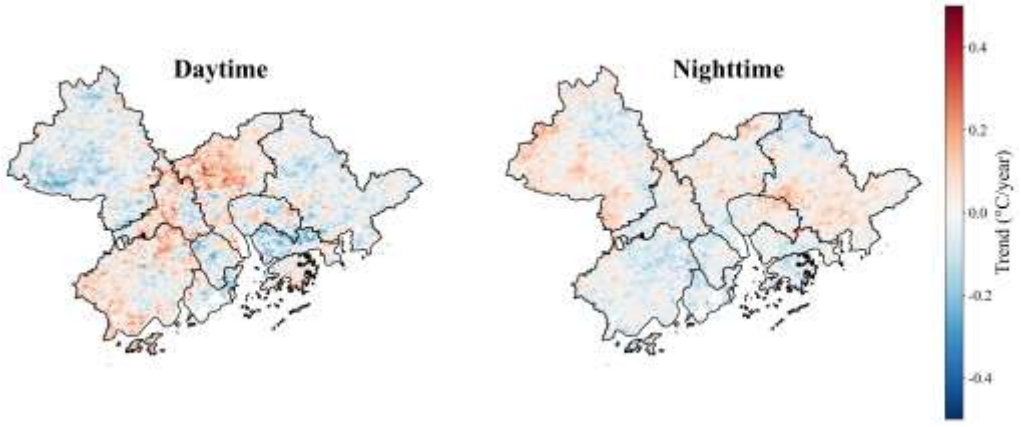

Fig.5 Daytime and Nighttime SUHI Trend Chart

Table 6 Statistical Characteristics of SUHI during Daytime and Nighttime from 2018 to 2024

Year	Daytime Average SUHI	Nighttime Average SUHI	Daytime strong SUHI ratio	Nighttime strong SUHI ratio
2018	-0.03±1.82	-0.03±1.74	6.73%	0.97%
2019	-0.03±1.90	-0.02±1.34	7.88%	0.49%
2020	-0.03±2.00	-0.02±1.60	7.58%	0.92%
2021	-0.03±1.97	-0.02±1.57	7.83%	1.84%
2022	-0.03±2.10	-0.02±1.37	9.69%	0.55%
2023	-0.03±1.92	-0.02±1.45	7.50%	0.63%
2024	-0.03±1.74	-0.02±1.28	4.58%	0.42%

Note: SUHI refers to Standardized Surface Urban Heat Island Intensity, which is calculated by subtracting the regional mean land surface temperature (LST) from the LST of each spatial unit and dividing the result by the regional standard deviation. A positive SUHI value indicates that the temperature of a given area is higher than the regional average, whereas a negative value indicates that it is lower than the regional average. The proportion of strong heat island areas refers to the percentage of pixels with SUHI values >1 relative to the total number of pixels within the study area. Because SUHI is derived using Z-score standardization, its regional mean theoretically approaches zero. Therefore, this study primarily focuses on spatial variation characteristics and changes in the proportion of strong heat island areas.

3.2 Spatial Aggregation Characteristics of Daytime and Nighttime SUHI

To reveal the spatial aggregation patterns and the distribution of hotspots and cold spots of daytime and nighttime SUHI Intensity in the GBA, this study employed Global Moran's I and Local Indicators of Spatial Association (LISA) to analyze SUHI data from 2018 to 2024. The results indicate that both daytime and nighttime SUHI exhibited significant positive spatial autocorrelation throughout the study period (daytime Moran's I: 0.936–0.946; nighttime Moran's I: 0.958–0.975), with corresponding Z-scores exceeding 162 and p-values below 0.0001 (Table 7). These findings confirm that the thermal environment of the study area was not randomly distributed but exhibited pronounced spatial clustering. The high Moran's I values indicate strong positive spatial autocorrelation of SUHI, which may be attributed to the spatial continuity of thermal landscapes and relatively homogeneous thermal characteristics at the urban agglomeration scale, which may be attributed to the spatial continuity of thermal landscapes and the relatively homogeneous thermal characteristics at the urban agglomeration scale. High-temperature areas tend to cluster with neighboring high-temperature areas, while low-temperature areas are spatially aggregated with other low-temperature areas, indicating strong spatial dependence and persistence of the thermal environment across the GBA.

According to the local spatial autocorrelation results (Figure 6), High–High clusters were predominantly distributed within the built-up areas of core cities in the Pearl River Delta, including the central urban areas of Guangzhou, the metropolitan core of Shenzhen, the manufacturing-intensive Dongguan–Foshan region, and the Guangzhou–Shenzhen–Hong Kong development corridor. These areas are characterized by highly contiguous impervious surfaces, intensive population and industrial activities, and substantial anthropogenic heat emissions, resulting in stable and persistent heat island hotspots. In contrast, Low–Low clusters were mainly distributed in the northern mountainous ecological barrier regions and coastal water bodies, including forested areas such as Conghua and Longmen, as well as coastal waters around the Pearl River Estuary and Lingdingyang. Benefiting from dense vegetation cover and extensive water surfaces, these areas exhibit strong evapotranspiration and water-cooling effects, thereby forming persistent and stable cold island clusters. Overall, the thermal environment of the GBA exhibits a spatial differentiation pattern characterized by "urban heating in the center and ecological cooling in the periphery."

A comparison between daytime and nighttime conditions revealed that Moran's I values were generally higher at night than during the daytime, indicating stronger spatial continuity and clustering of the nighttime thermal environment. During the daytime, solar radiation, land-cover characteristics, and local environmental heterogeneity contribute to differences in regional heating rates, resulting in relatively high spatial variability. At

night, however, in the absence of solar radiation, heat stored in urban built-up areas is gradually released from buildings, roads, and other impervious surfaces, leading to a more uniform spatial diffusion and accumulation of heat and thereby strengthening thermal spatial correlation. Furthermore, nighttime hotspot areas were spatially more compact (Figure 7), being concentrated in the urban cores of Guangzhou and Shenzhen and their surrounding built-up areas, whereas cold spots remained stable within the northern mountainous regions and coastal waters. These findings suggest that urban heat storage plays a crucial role in sustaining nighttime heat island effects. Therefore, although the daytime and nighttime thermal environments share a broadly similar spatial structure, they exhibit distinct spatial organization characteristics.

Table 7 Spatial Autocorrelation Statistics of Daytime and Nighttime SUHI from 2018 to 2024

Year	Daytime Moran's I	Daytime Z-value	Daytime p-value	Nighttime Moran's I	Nighttime Z value	Nighttime P value
018	0.9358	162.80	<0.0001	0.9583	166.72	<0.0001
2019	0.9402	163.56	<0.0001	0.9665	168.15	<0.0001
2020	0.9419	163.86	<0.0001	0.9745	169.53	<0.0001
2021	0.9427	164.01	<0.0001	0.9731	169.30	<0.0001
2022	0.9455	164.50	<0.0001	0.9638	167.68	<0.0001
2023	0.9460	164.58	<0.0001	0.9742	169.49	<0.0001
2024	0.9427	164.01	<0.0001	0.9600	167.02	<0.0001

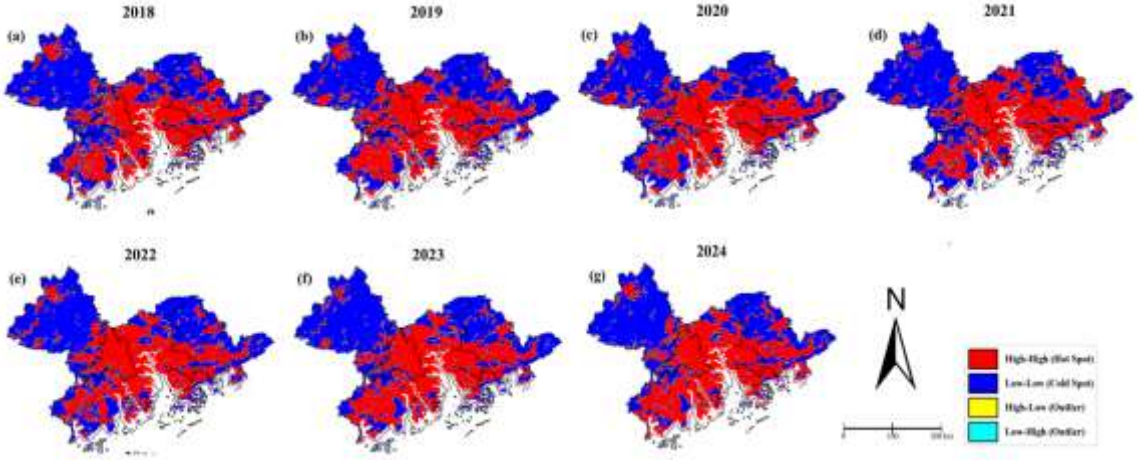

Figure 6 Daytime SUHI LISA Cluster Map

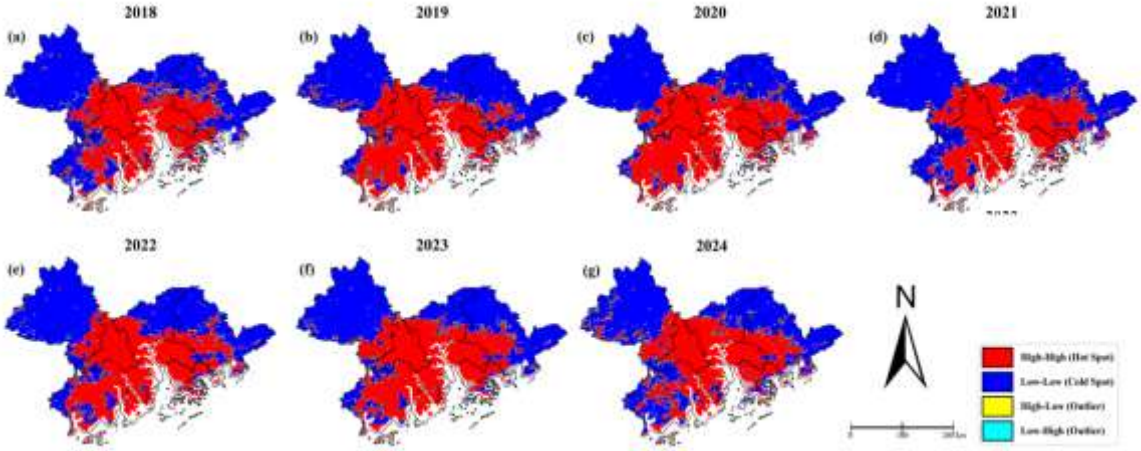

Fig.7 Nighttime SUHI LISA Cluster Map

3.3 Land-Use Transitions and Their Impacts on SUHI

To reveal the influence of different land-use change types on the urban surface thermal environment during the study period, this study conducted a statistical analysis of various land-use transition processes based on the land-use transition matrix. The relationship between land-use change and thermal environmental response was further explored by integrating changes in SUHI (ΔSUHI) under different transition pathways.

The results of the land-use transition matrix indicate that land-use change from 2018 to 2024 was primarily characterized by the expansion of built-up land (Figure 8). Within the effective analysis region, stable built-up land occupied the largest proportion, accounting for 69.14% of the analyzed area, indicating that urban built-up areas continued to dominate the regional land-use pattern (Table 8). Apart from stable built-up land, major land-use transitions involved the conversion of ecological spaces (e.g., cropland, forest, water bodies, and wetlands) into built-up land, reflecting the significant impact of urban expansion on regional land-cover patterns during the study period (Figure 9).

From the perspective of the relationship between land-use transition pathways and SUHI responses, different surface transformation types exhibited distinct effects. The conversion of ecological spaces into built-up land generally resulted in positive ΔSUHI values, indicating an increase in surface temperature following land-use change. This suggests that increases in impervious surface coverage, reductions in vegetation cover, and alterations in surface energy exchange processes exacerbate the urban heat island effect (Table 8). Notably, the warming effect was most pronounced when water bodies and wetlands were converted into built-up land, with ΔSUHI reaching relatively high levels. This finding indicates that these blue spaces, as critical regional cooling sources, experienced weakened evapotranspiration cooling and thermal regulation functions during the conversion process, resulting in substantial local thermal environmental deterioration (Figure 10). These results further highlight that the loss of water bodies and wetlands not only alters the regional landscape pattern but also reduces the thermal buffering capacity of urban ecosystems.

In contrast, the conversion of cropland into built-up land also produced a warming effect; however, the magnitude of ΔSUHI was lower than that associated with the conversion of water bodies and wetlands (Table 8). This may be attributed to the inherent vegetation cover and moisture regulation capacity of cropland. Although its ecological regulation functions decline following conversion, the resulting loss of cooling capacity is relatively limited compared with that of water bodies and wetlands. Therefore, different types of ecological spaces exhibit varying thermal environmental responses during urban expansion, with the loss of major cooling-source spaces exerting a more direct influence on SUHI intensification.

In addition, some land-use transition pathways exhibited cooling effects. For example, when built-up land was converted into ecological spaces such as green spaces, forests, or water bodies, ΔSUHI values became negative, indicating that ecological restoration, urban renewal, and blue–green space development can effectively reduce surface temperatures (Table 8). These transition pathways regulate the urban thermal environment by increasing vegetation cover, enhancing evapotranspiration, and optimizing urban surface structures. Spatially, cooling-oriented land-use transitions were concentrated in urban renewal areas and peripheral ecological optimization zones, highlighting the importance of land-use structure adjustment in mitigating SUHI (Figure 9).

In summary, land-use change in the Pearl River Delta region was primarily driven by urban expansion, with the continuous increase in built-up land representing the dominant pathway influencing SUHI variations (Figure 10). Different land-use transition types exerted markedly different effects on the thermal environment: transitions from ecological spaces to built-up land generally intensified SUHI, whereas ecological restoration and the expansion of blue–green spaces generated cooling effects (Table 8). Therefore, future urban development should prioritize the protection of highly efficient cooling sources, particularly water bodies and wetlands. By increasing the proportion of ecological land and optimizing land-use structures, a more balanced coordination between urban expansion and thermal environmental regulation can be achieved.

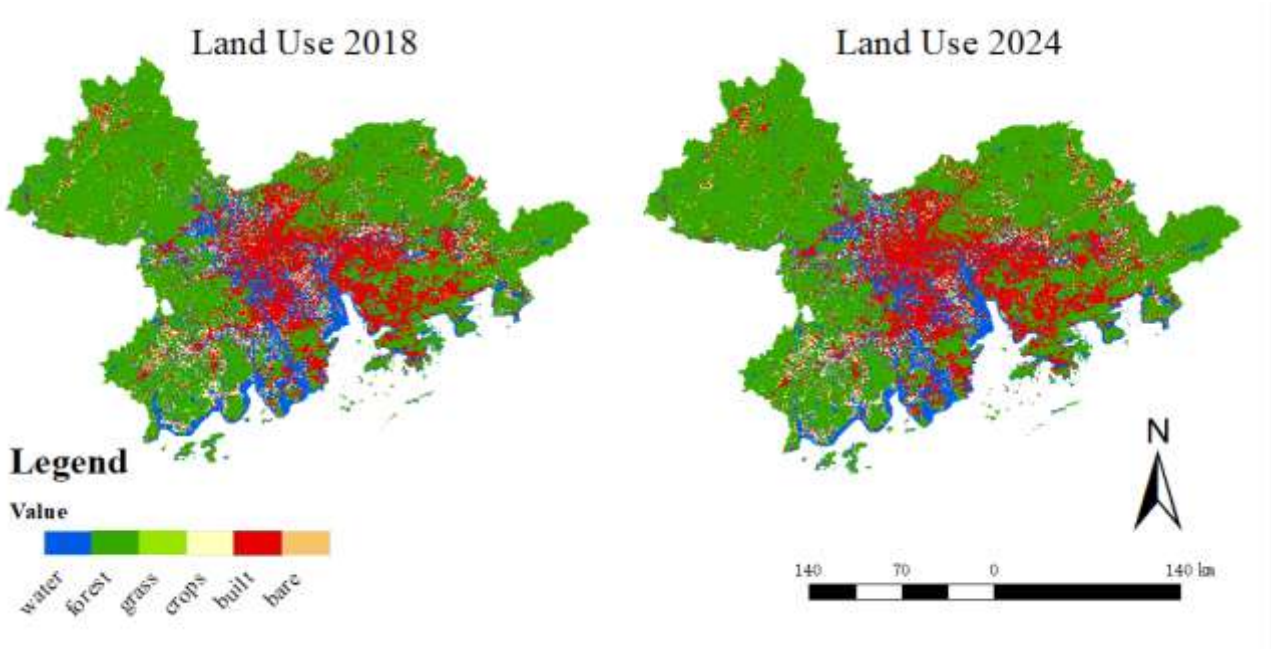

Fig.8 Land Use Maps for 2018 and 2024

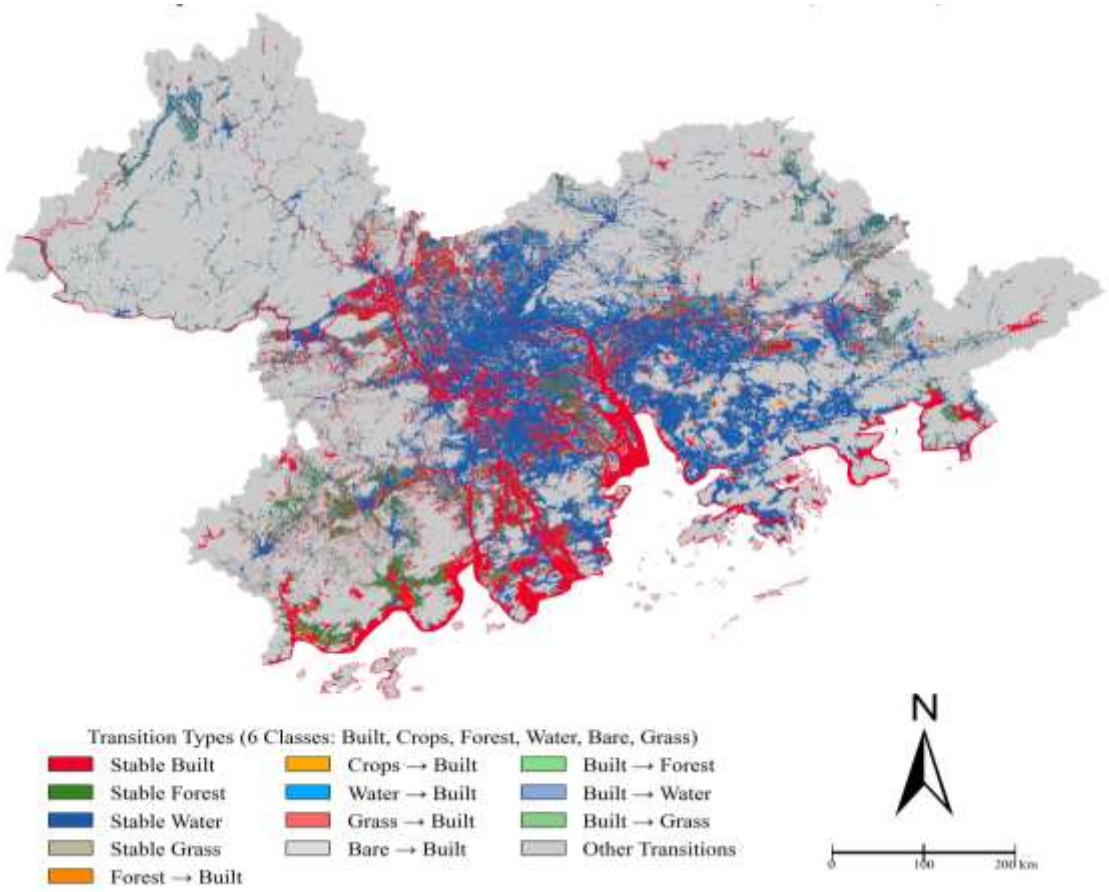

Fig.9 Spatial Distributions of Land Use Transfers in GBA (2018-2024)

Table 8 Land Use Transfer Types and SUHI Response from 2018 to 2024

Transfer Type	Area/Ratio	Average ΔSUHI_Day	Average ΔSUHI_Night	Explanation
Forestland →Built-up land	5.15 km² (0.46%)	+4.29	+5.29	Conversion of ecological space to construction land
Cropland →Built-up land	16.15 km² (1.45%)	+2.60	+2.99	Urban expansion process
Water body →Built-up land	17.82 km² (1.60%)	+4.99	+5.97	Reduction of cooling sources
Built-up Land →Green space	37.00 km² (3.32%)	-4.07	-5.08	Ecological restoration or renovation
Stable Built-up land	769.87 km² (69.14%)	+0.30	+0.30	High Heat Island Retention Zone
Stable Forestland/Water bodies	267.47 km² (24.02%)	+0.10	+0.11	Cold Island Maintenance Zone

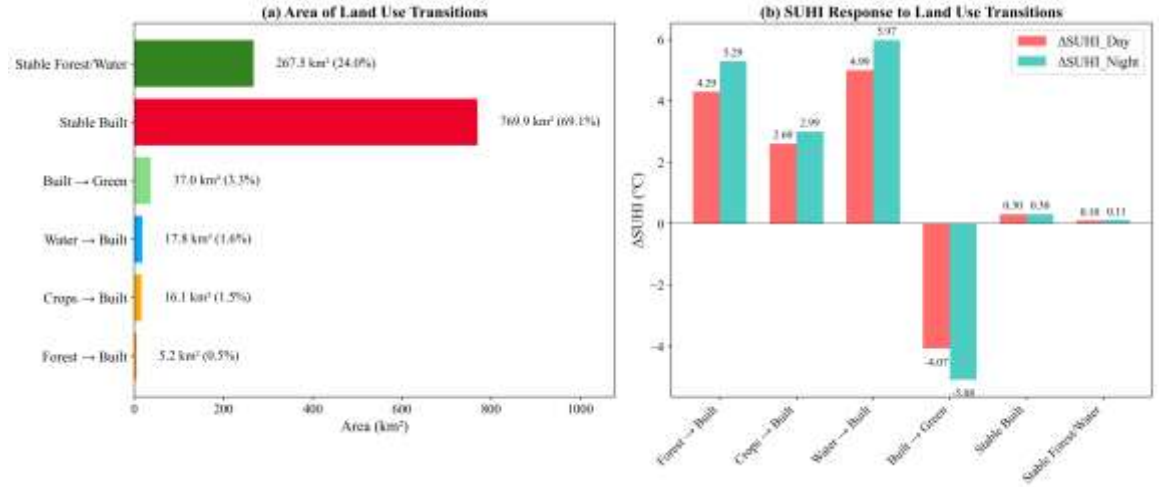

Fig.10 Bar chart of daytime and nighttime ΔSUHI under different land-use transfer types

3.4 Key Drivers of Daytime and Nighttime SUHI

To identify the primary drivers and underlying mechanisms of daytime and nighttime SUHI Intensity in the GBA, this study conducted a contribution analysis of natural environmental and socioeconomic variables using the XGBoost model and SHAP method. The results indicate that both daytime and nighttime SUHI are influenced by land-cover characteristics and human activities; however, their dominant driving factors and influence magnitudes differ substantially (Tables 9 and 10).

The primary drivers of daytime SUHI include the NDBSI, NDVI, NDMI, MNDWI, and NTL (Figure 11). Among these variables, NDBSI exhibits the highest importance, with SHAP values generally indicating positive contributions. This suggests that increases in impervious surface coverage and the expansion of built-up areas enhance the capacity for heat absorption and storage, thereby intensifying the heat island effect. In contrast, NDVI, NDMI, and MNDWI exhibit significant negative contributions indicating that increased vegetation cover, improved moisture conditions, and expanded water bodies can effectively mitigate the heat island effect through evapotranspiration cooling, water-related thermal regulation, and heat dissipation processes (Figure 13). Overall, the daytime thermal environment is primarily governed by land-cover characteristics and ecological conditions, with differences in surface energy balance among various underlying surfaces representing a key factor driving spatial thermal variability.

For nighttime SUHI, the key driving factors include NDBSI, NTL, population density (PD), GDP, and NDVI (Figure 12). NDBSI remains highly influential, confirming that built-up areas and impervious surfaces constitute the common physical basis of both daytime and

nighttime heat island effects. Meanwhile, the importance of NTL, PD, and GDP increases substantially, with SHAP values predominantly indicating positive contributions. This suggests that nighttime heat islands are influenced not only by urban heat storage effects but also by population concentration, economic activities, and anthropogenic heat emissions. High-density urban areas continuously release heat accumulated during the daytime, while anthropogenic heat generated from transportation, commercial activities, and energy consumption further intensifies local warming, resulting in more pronounced nighttime heat island effects.

In terms of variable importance rankings, land-cover characteristics dominate daytime SUHI, whereas nighttime SUHI is more strongly influenced by the intensity of human activities and the level of urbanization (Figure 13). These findings highlight a significant difference in the formation mechanisms of daytime and nighttime thermal environments in the GBA. Daytime thermal conditions are primarily controlled by solar radiation and underlying surface properties, whereas nighttime thermal conditions reflect the combined effects of heat release and anthropogenic heat emissions. Overall, urban expansion and increasing impervious surface coverage are key drivers of heat island intensification, while enhancing vegetation cover, protecting water bodies, and optimizing urban ecological structures represent critical strategies for mitigating regional thermal environmental problems.

Table 9 Evaluation Results of XGBoost Model Prediction Accuracy

indicator	Daytime SUHI	Nighttime SUHI
R^2	0.785	0.812
RMSE	0.523	0.456
MAE	0.387	0.342

Table 10 Ranking of Key Influencing Factors for Daytime and Nighttime SUHI

Sorting	Daytime SUHI key factor	Direction of action	Nighttime SUHI key factor	Direction of action
1	NDBSI	Positive	NDBSI	Positive
2	NDVI	Negative	NTL	Positive
3	NDMI	Negative	PD	Positive
4	MNDWI	Negative	GDP	Positive
5	NTL	Positive	NDVI	Negative

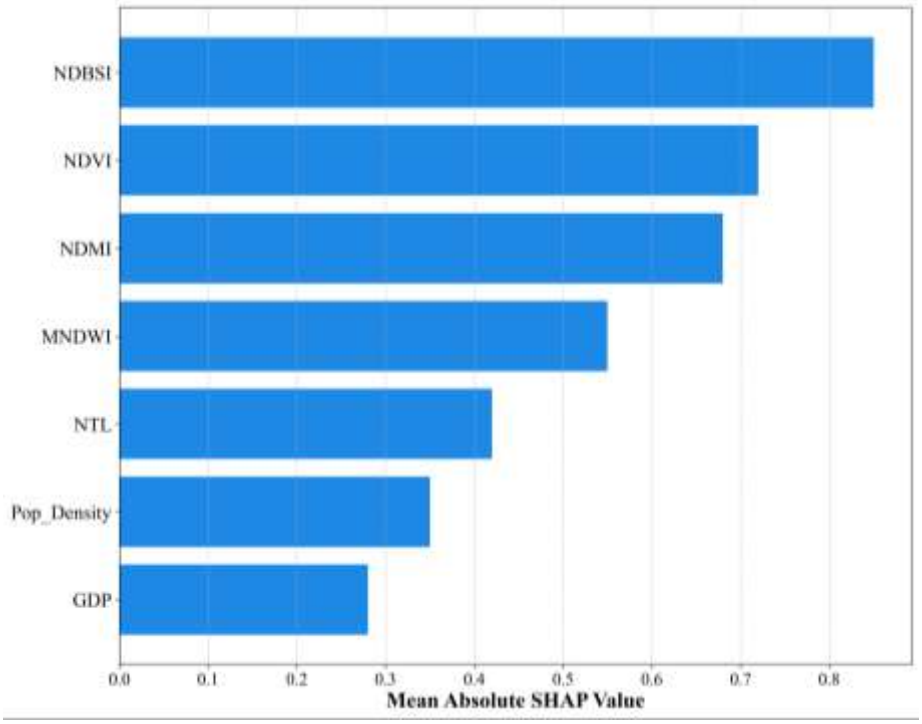

Fig.11 SHAP Summary Plot of Daytime SUHI

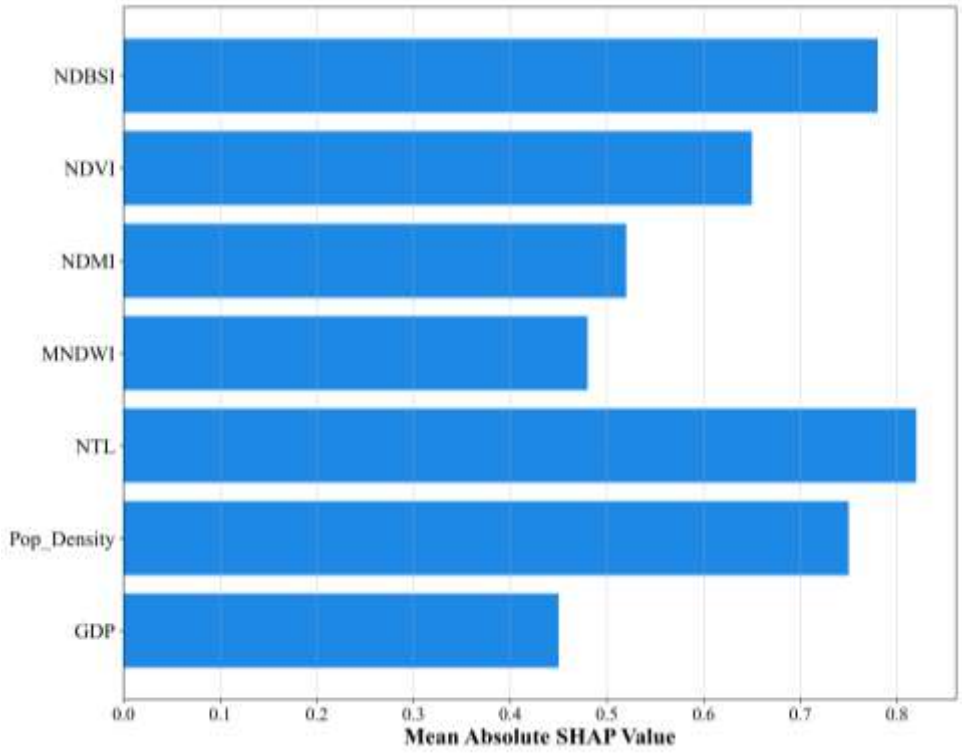

Fig.12 SHAP Summary Plot of Nighttime SUHI

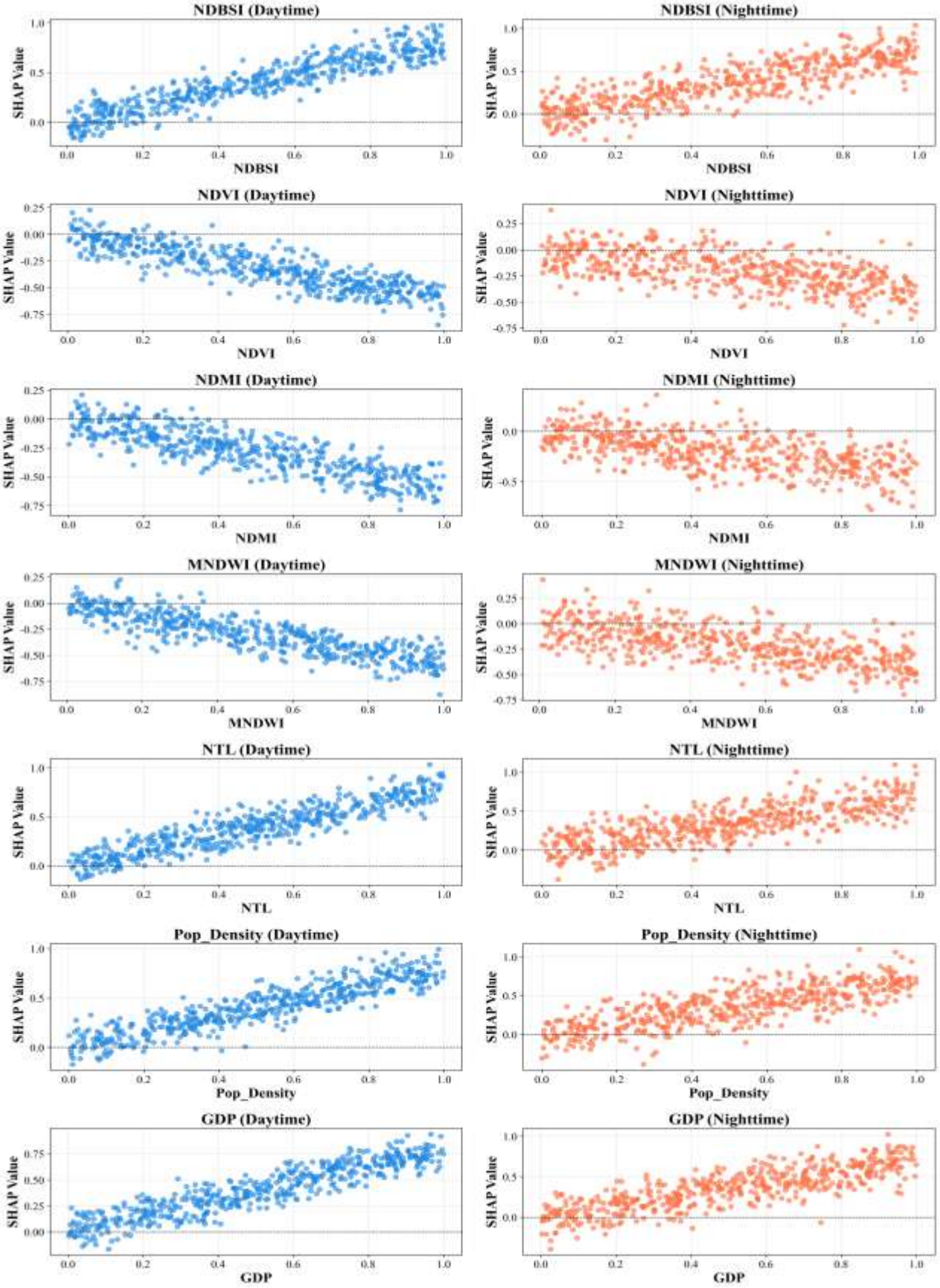

Fig.13 SHAP Dependence Plots of Key Variables

IV. DISCUSSION

4.1 Differences and Mechanisms of Daytime and Nighttime SUHI

The formation mechanisms of daytime and nighttime SUHI exhibit distinct differences. This study found that daytime SUHI is primarily influenced by NDBSI, NDVI, NDMI, and MNDWI, with NDBSI showing a significant positive contribution, whereas NDVI, NDMI, and MNDWI exhibit significant negative contributions. These findings indicate that increased surface hardening and the reduction of ecological cooling sources are key drivers of daytime heat island formation. In contrast, nighttime SUHI is mainly influenced by NDBSI, NTL, population density, and GDP, suggesting that nighttime heat islands are associated not only with surface heat storage but also with population agglomeration, anthropogenic heat emissions, and urban economic activities. The results further reveal that NDVI and MNDWI exert significant negative effects on daytime SUHI, highlighting the important roles of vegetation cover and water distribution as ecological factors in mitigating thermal environmental stress.

4.2 Implications of Land-Use Change for Thermal Environmental Variations

Land-use change is not merely a shift in land-use categories but also a surface process that drives thermal environmental evolution. The conversion of ecological spaces into built-up areas typically results in reduced vegetation cover, deteriorated water conditions, increased impervious surface coverage, and enhanced surface heat storage, thereby contributing to higher SUHI intensity. Conversely, the conversion of built-up areas into green spaces, water bodies, or other ecological spaces can enhance evapotranspiration and water-cooling effects, thereby reducing SUHI intensity. The results indicate that the conversion of water bodies/wetlands, forests, and cropland into built-up areas constituted the primary warming pathways during the study period (Table 8). Among these pathways, the conversion of water bodies/wetlands into built-up areas exhibited the strongest warming effect, with daytime and nighttime ΔSUHI reaching 4.99 and 5.97, respectively. In contrast, the conversion of built-up areas into green spaces or water bodies generated significant cooling effects, reducing daytime and nighttime ΔSUHI by 4.07 and 5.08, respectively. These findings highlight the importance of blue–green space restoration in mitigating heat island effects. The thermal impacts of land-use change exhibit clear path dependency, with different transition pathways producing varying degrees of thermal response. Notably, the warming effects resulting from the loss of ecological spaces generally exceed those associated with structural adjustments within built-up areas.

4.3 Planning Implications Derived from Key Driving Factors

The value of the XGBoost-SHAP framework lies not only in improving prediction accuracy but also in identifying the variables that are most important in explaining variations in heat island intensity.The positive contribution of NDBSI to SUHI highlights the importance of reducing surface hardening, improving impervious surface materials, and increasing permeable pavements. If NDVI, NDMI, or MNDWI show negative contributions, enhancing vegetation cover, maintaining surface moisture, and protecting blue–green spaces become essential strategies for mitigating heat island effects. Furthermore, if NTL, population density, or GDP contribute substantially to nighttime SUHI, greater attention should be directed toward managing anthropogenic heat emissions, transportation-related activities, and thermal conditions in high-intensity urban functional zones.

From the perspective of urban planning and environmental management, reducing surface hardening and enhancing blue–green space connectivity should be prioritized in thermal environment governance across the Guangdong–Hong Kong–Macao Greater Bay Area to achieve a balance between urban expansion and ecological conservation. Three key strategies are proposed: (1) **Priority Cooling Zones in Heat Island Hotspots**, involving measures such as cool roofs, increased shading vegetation, reduced continuous impervious surfaces, and improved urban ventilation; (2) **Thermal Risk Control Zones in Urban Expansion Areas**, emphasizing controlled development intensity, the preservation of ecological buffer zones, and increased proportions of green and permeable surfaces; and (3) **Blue–Green Ecological Cooling Source Protection Zones**, focusing on the protection of forests, water bodies, wetlands, and blue–green corridors to prevent landscape fragmentation (Table 11).

Table 11 Zoning Thermal Environment Management and Optimization Recommendations

Governance Zones	Basis for identification	Recommended measures
Priority Cooling Zone for UHI Hotspots	SUHI>1 or LISA High-High	Cool roofs, increased greenery and shading, reduced continuous hardened surfaces, improved ventilation
Urban Expansion Heat Risk Control Zone	Non-buildup land → Buildup land and ΔSUHI > 0	Control development intensity, preserve ecological buffer zones, and increase green space and permeable surface ratios
Blue-Green Ecological Cold Source Conservation Zone	Low SUHI with higher NDVI/NDWI/MNDWI	Protect forests, water bodies, wetlands, and blue-green corridors to prevent fragmentation

4.4 Research Limitations

This study has several limitations. First, although MODIS LST data are suitable for urban agglomeration-scale analyses, their spatial resolution is insufficient to capture thermal environmental variations at the neighborhood scale. Second, socioeconomic variables such as population density and GDP were derived from administrative statistics and subsequently assigned spatially within the model, which may not adequately reflect fine-scale spatial variability at the pixel level. Third, although the XGBoost-SHAP framework provides statistical interpretations and quantifies the contributions of explanatory variables, it cannot establish strict causal relationships. Fourth, spatial heterogeneity and pathway-based analytical approaches were not incorporated into this study, limiting the exploration of local mechanisms and direct or indirect influence pathways.

V. CONCLUSIONS

This study constructed daytime and nighttime SUHI Intensity indicators for the Guangdong–Hong Kong–Macao Greater Bay Area (GBA) from 2018 to 2024 using multi-source spatial data. Spatiotemporal statistical analysis, spatial autocorrelation analysis, land-use transition matrices, and the XGBoost-SHAP framework were employed to investigate the spatiotemporal evolution of SUHI, its response to land-use changes, and its key driving factors. The main conclusions are as follows:

(1) Daytime and nighttime SUHI exhibited significant spatial heterogeneity. High-SUHI areas were concentrated in the core built-up regions of the Pearl River Delta, including Guangzhou, Shenzhen, Dongguan, and Foshan, whereas low-SUHI areas were primarily distributed in the northern mountainous forest regions and coastal water bodies such as the Pearl River Estuary and Lingdingyang. During the study period, SUHI anomaly increased along the Shenzhen–Dongguan–Huizhou urban development corridor but weakened or remained stable in the northwestern mountainous regions, including Zhaoqing.

(2) The results of Global Moran's I and LISA revealed significant spatial clustering of SUHI. High–High hotspot clusters were primarily distributed within the core built-up areas of Guangzhou, Shenzhen, Dongguan, Foshan, and the Guangzhou–Shenzhen–Hong Kong development corridor, whereas Low–Low cold spot clusters were concentrated in the northern ecological conservation areas and the coastal waters of the Pearl River Estuary.

(3) Land-use transitions played a critical role in SUHI dynamics. The conversion of forests, cropland, and wetlands into built-up areas resulted in pronounced warming effects, whereas transitions from built-up areas to green spaces or water bodies significantly mitigated the urban heat island effect.

(4) XGBoost-SHAP analysis identified NDBSI, NDVI, NDMI, MNDWI, and NTL as the primary drivers of daytime SUHI, whereas NDBSI, NTL, PD, GDP, and NDVI were identified as the dominant drivers of nighttime SUHI. Built-up and dry surface characteristics generally intensified SUHI, whereas vegetation cover and surface moisture conditions contributed to its mitigation.

(5) Thermal environment governance in the GBA should prioritize heat island hotspot cooling zones, urban expansion risk-control areas, and blue–green ecological cooling-source protection zones, while adopting differentiated management strategies for daytime and nighttime thermal conditions. Future efforts should integrate "blue–green space conservation–urban expansion regulation–targeted hotspot is cooling" to promote a balance between urban development and ecological protection.

From a theoretical perspective, this study established an integrated framework encompassing SUHI pattern identification, land-use transition responses, and mechanistic interpretation from a diurnal perspective,

thereby enriching thermal environment research at the urban agglomeration scale. From a practical perspective, the findings provide scientific support for territorial spatial planning, urban expansion management, and blue–green space optimization in the GBA.

REFERENCES

[1] Chen, T. Q., and Guestrin, C. XGBoost: A scalable tree boosting system, Proceedings of the 22nd ACM SIGKDD International Conference on Knowledge Discovery and Data Mining. New York: ACM, 2016: 785-794.

[2] Chen, X. L., Zhao, H. M., Li, P. X., et al. Remote sensing image-based analysis of the relationship between urban heat island and land use/cover changes. Remote Sensing of Environment, 2006, 104(2): 133-146.

[3] Li, X. X., Zhou, Y. Y., Asrar, G. R., et al. Response of vegetation and surface water to urban thermal environment and implications for heat mitigation. Science of the Total Environment, 2020, 703: 134706.

[4] Liu J Y, Kuang W H, Zhang Z X, et al. Spatiotemporal characteristics, patterns and causes of land-use changes in China since the late 1980s. Journal of Geographical Sciences, 2014, 24(2):195-210.

[5] Lundberg, S. M., and Lee, S. I. A unified approach to interpreting model predictions, Proceedings of the 31st International Conference on Neural Information Processing Systems. Long Beach: NIPS, 2017: 4768-4777.

[6] Oke, T. R. Boundary Layer Climates. 2nd ed. London: Routledge, 1987.

[7] Pontius, R. G., Shusas, E., & McEachern, M. Detecting important categorical land changes while accounting for persistence. Agriculture, Ecosystems & Environment, 2004, 101(2-3), 251-268.

[8] Wang, Y. H., Zhang, H. Y., Liu, Z. Q., et al. Spatial clustering characteristics and driving mechanisms of urban heat island effects in the Guangdong-Hong Kong-Macao Greater Bay Area. Journal of Geo-information Science, 2023, 25(8): 1578-1593.

[9] Yang, J., Wang, Y. H., Xiu, C. L., et al. Exploring nonlinear relationships between urban heat island intensity and driving factors using machine learning approaches. Sustainable Cities and Society, 2022, 81: 103838.

[10] Zhou, D. C., Zhao, S. Q., Liu, S. G., et al. Surface urban heat island in China's 32 major cities: Spatial patterns and drivers. Remote Sensing of Environment, 2017, 152: 51-61.